Journal of Instrumentation

TECHNICAL REPORT

First investigation of coherent terahertz radiation at a Super Tau Charm Factory

To cite this article: W.W. Gao *et al* 2022 *JINST* **17** T01006

View the article online for updates and enhancements.

PUBLISHED BY IOP PUBLISHING FOR SISSA MEDIALAB

RECEIVED: *October 11, 2021*
REVISED: *January 12, 2022*
ACCEPTED: *January 12, 2022*
PUBLISHED: *January 31, 2022*

TECHNICAL REPORT

First investigation of coherent terahertz radiation at a Super Tau Charm Factory

W.W. Gao,[a,*] J.Q. Lan,[a] F.Y. Zhao[a] and Q. Luo[b]

[a] *School of Electronic, Electrical Engineering and Physics, Fujian University of Technology, South Xuefu road, Fuzhou 350118, China*

[b] *National Synchrotron Radiation Laboratory, University of Science and Technology of China, South Hezuohua road, Hefei 230026, China*

E-mail: gaoww@ustc.edu.cn

ABSTRACT: The coherent THz radiation with long-short beam operation mode is discussed at a Super Tau Charm Factory. The beam dynamics, RF parameters and some important issues are given. Two version of short bunch length are designed. Results show that the 2.0 mm short bunch length correspond to the frequency where the radiation power decreased sharply. The short bunch length should minimized to smaller than 1.5 mm at this facility to achieve proper coherent radiation power at THz frequency region.

KEYWORDS: Accelerator modelling and simulations (multi-particle dynamics, single-particle dynamics); Beam dynamics

*Corresponding author.

https://doi.org/10.1088/1748-0221/17/01/T01006

2022 JINST 17 T01006

Contents

1 Introduction

Terahertz (THz) wave, which lies between millimeter wave and far-infrared region, is at the interface of electronics and photonics. The corresponding wavelength of THz is at the order of millimeter to sub millimeter range.

The THz wave can be used in the integrated circuits and THz communication, which has advantage in realization of integrated, low-cost, high speed, on-chip data communications [1, 2]. The Terahertz wave has, in particular, provided a method of terahertz atom probe microscopy, allowing new platform for microscopy with atomic spatial resolution. Compared to the ordinary microscopes, the THz circumvents the diffraction limit, even at these long wavelengths, the properties of materials can be probed on a nanometer scale [3, 4]. THz technology is also widely used in biology and medicine [5], with significant advantages in nondestructive testing. Recently, the THz-driven acceleration has emerged as a new way for delivering electron beam in a compact setup [6].

Free-electron lasers and fast diodes can produce narrow-band THz radiation. While, broadband THz radiation can be produced by thermal sources and table-top laser-driven sources [7] as well as by electron bunches in synchrotron accelerators [8].

The particles in a bunch traveling on a curved trajectory in free space emit synchrotron radiation with a broad spectrum of wavelengths. When the wavelengths comparable to the bunch length, the radiation from various particles is coherent, giving a radiated power proportional to the square of the particle population. This means that, if the electron bunch length of the circular accelerator is comparable to the THz wave length, coherent THz radiation can be achieved from the bending

2022 JINST 17 T01006

magnets. In this paper we will report the feasibility of coherent THz generation using ultra short electron bunches at a Super Tau Charm Factory (STCF) in synchrotron mode.

This STCF planning in China is a double ring circular collider with center mass energy range 2–7 GeV. This facility is designed to use large Piwinsky angle and crab waist sextupole scheme to increase the luminosity. In order to meet the requirement of large Piwinsky angle and crab waist collision scheme long bunch length is required. At the 2 GeV optimized energy of collision mode the bunch length should be 1.2 cm and should be flexibly adjusted at other energies [9]. Especially, the bunch length should be flexibly modified to change the beam-beam parameters when the betatron function at the collision point is changed. Therefore, harmonic cavities are preferred to adjust the bunch length at this STCF. In order to effectively utilize these harmonic cavities, we plan to design a long-short bunch operation mode at the synchrotron radiation mode with 1 GeV. In this mode the short bunch length should be minimized to smaller than 3 mm to achieve coherent THz radiation in theory.

In this paper, we will give the related physical design of the coherent synchrotron radiation pulse at the THz regime in this STCF project. Simulation and theoretical work of the long-short bunch length operation mode is presented. The paper is organized as the following. In section 2 the bunch length formula with harmonic cavities are given. In section 3 the coherent THz radiation mode design process is detailedly presented. In subsection 3.1 some sections of the STCF lattice are redesigned to meet the requirement of the THz mode. In subsection 3.2 the harmonic cavities are carefully chosen for long-short bunch length operation. In subsection 3.3 the bunch length evolution process at the long-short beam operation mode is numerically tracked. In section 4 the corresponding issues of the long-short bunch length mode are given. At the last section the summary and the outlook are given.

2 Bunch length formula with multiple cavities

The bunch length formula with a single RF cavity can be expressed as the following [10].

$$\sigma_z = \sqrt{\frac{2\pi C_q}{(mc^2)^2}\frac{\alpha R}{J_\epsilon \rho}\frac{E^3}{eV'}}. \tag{2.1}$$

where $C_q = 3.84 \times 10^{-13}$m is the quantum constant, α is the momentum compaction factor, $R = L/2 \times \pi$ is the radius of the design orbit, E is the nominal energy, m and e are the rest mass and the charge of the accelerated electron, c is the velocity of the light, ρ is the bending radius, J_ϵ is the longitudinal damping partition number, V' is the voltage gradient where the particle come across.

However, in a storage ring with several RF cavities the bunch length formula is shown as the follows [11], for the sake of simplicity we assume that all of the RF cavities are installed at one position with zero length.

$$\sigma_z = \frac{h\eta\omega_0}{\Omega_s}\delta_p. \tag{2.2}$$

where h is the harmonic number, η is the phase slip factor, $\omega_0 = \frac{\beta c}{R}$ is the angular revolution frequency, δ_p is the rms momentum deviation. Ω_s is the new synchrotron tune with several RF cavities and can be expressed as follows,

$$\Omega_s = \sqrt{\left| -\frac{h\omega_0^2\eta}{\beta^2 E} \sum_i \frac{eV_i}{2\pi} \cos\phi_s(\theta_i) \right|}. \tag{2.3}$$

here, V_i is the i-th RF cavity voltage, $\phi_s(\theta_i)$ is the synchrotron phase of the i-th RF cavity, β is the velocity of the electron in unit of c.

From equation (2.3), we see that the bunch length has a close relationship to the voltage gradient and momentum compaction factor. The momentum compaction factor, which mainly determined by bending radius of dipole magnets and dispersion function, is determined by lattice structure and the geometry of the storage ring. In the case that the lattice structure cannot be changed much, it is very effective to use harmonic cavity to control the bunch length. Thus in this paper we use the harmonic cavities but not the momentum compaction factor to manipulate the bunch length. These harmonic cavities will increase the voltage gradient so as to shorten the bunch length at one position and decrease the voltage gradient so as to lengthen the bunch length at another position. So that the storage ring will be filled with interleaved long and short bunches. The short bunches will radiate coherent THz and the long bunches will increase the beam current.

3 Coherent THz radiation mode design at a STCF

3.1 STCF lattice design for THz radiation mode

The STCF requires ultra low betatron function, namely sub millimeter range at the interaction point for the collision mode to get high luminosity. The very low betatron function leads to that the maximum betatron function close to the interaction point nearly reaches to 2000 m [9]. However, in the THz radiation mode the maximum betatron function should be minimized to the tens of meters. As a result, the lattice of the interaction region should be redesigned. In this design the magnet positions remain unchanged, while merely the strengths of quadrupole are redesigned to meet the THz requirement.

In this new designed lattice, the betatron functions at the interaction point are $\beta_x = 25$ m and $\beta_y = 10$ m, and then the maximum betatron function of the interaction section is minimized to smaller than 55 m. In this design the local chromaticity correction scheme is not adopted but a few dispersion bumps are created for sextupole implementation. Additionally, the quadrupole strengths of the matching section between interaction and the arc region are adjusted to meet the connection requirement. The betatron function and dispersion function of the interaction region are plotted in figure 1. In this THz mode the arc section keeps the scheme used in the collision mode as reported in ref. [9].

Except the linear properties of the lattice mentioned above it also needs for good nonlinear beam performances. The most important nonlinear property is large enough dynamic aperture at the injection point for beam injection. Since the linear tunes have a close relationship on the dynamic aperture, we use the following matrix to replace the whole technical section to search for a reasonable working point to obtain a large dynamic aperture.

$$\begin{bmatrix} x \\ p_x \\ y \\ p_y \end{bmatrix}_1 = \begin{bmatrix} \cos(2\pi\nu_x) & \beta_x \sin(2\pi\nu_x) & 0 & 0 \\ -\sin(2\pi\nu_x)/\beta_x & \cos(2\pi\nu_x) & 0 & 0 \\ 0 & 0 & \cos(2\pi\nu_y) & \beta_y \sin(2\pi\nu_y) \\ 0 & 0 & -\sin(2\pi\nu_y)/\beta_y & \cos(2\pi\nu_y) \end{bmatrix} \begin{bmatrix} x \\ p_x \\ y \\ p_y \end{bmatrix}_0 \tag{3.1}$$

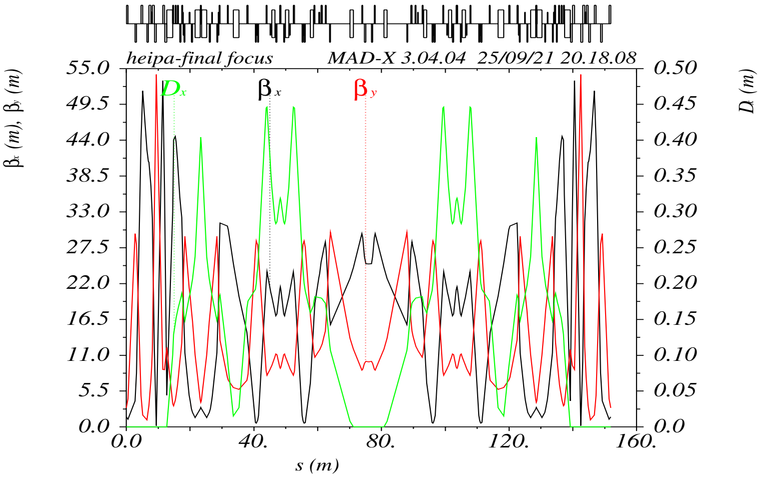

Figure 1. Optical function of the interaction region.

where x, y and p_x, p_y are the horizontal and vertical displacements from closed orbit and momentum deviations from synchrotron particle, ν_x and ν_y are the tunes of two transverse planes, β_x and β_y are the horizontal and vertical betatron functions.

By changing this matrix, the tune is changed and the corresponding dynamic aperture with different tune is tracked. The result of tune scan and the corresponding dynamic aperture area is plotted in figure 2. From figure 2 we see that the area A have a better dynamic aperture at both planes.

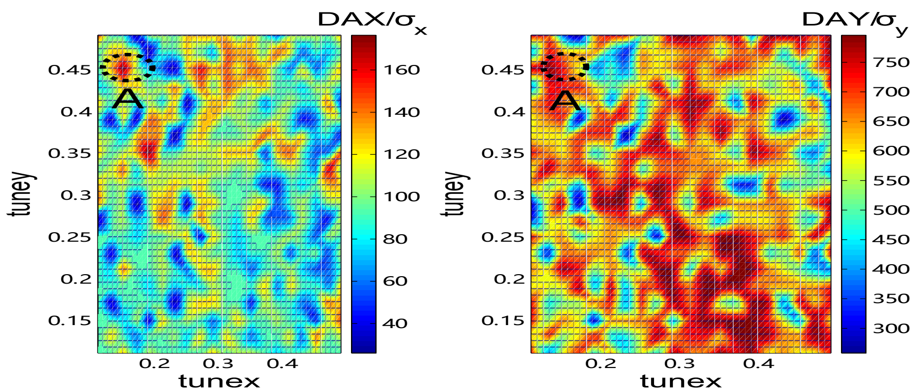

Figure 2. The relationship between dynamic aperture area and the tunes, the left plot draws the relations between horizontal dynamic aperture area and tunes, the right plot draws the relations between vertical dynamic aperture area and tunes.

Finally, we redesigned the lattice of the technical section and ensured that the tunes of the storage ring are $\nu_x = 35.151774$ and $\nu_y = 14.457221$, which corresponding to larger dynamic aperture area in figure 2. The beam optical functions of the new designed technical section satisfying the above tunes are plotted in figure 3. With these tunes, the strength of sextupole pairs at the arc section and the interaction region are varied to maximize the dynamic aperture with particle swarm optimization. The figure 4 shows the best dynamic aperture of the last generation.

2022 JINST 17 T01006

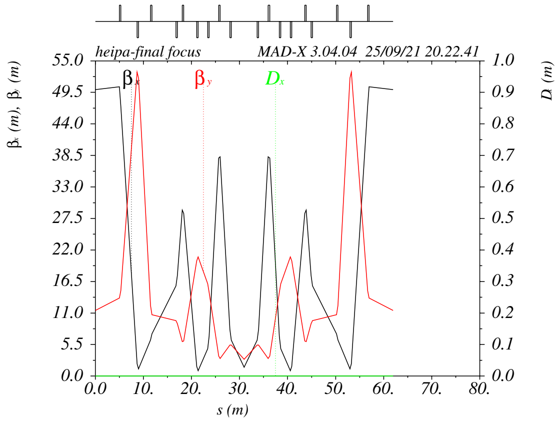

Figure 3. Optical function of the new technical section.

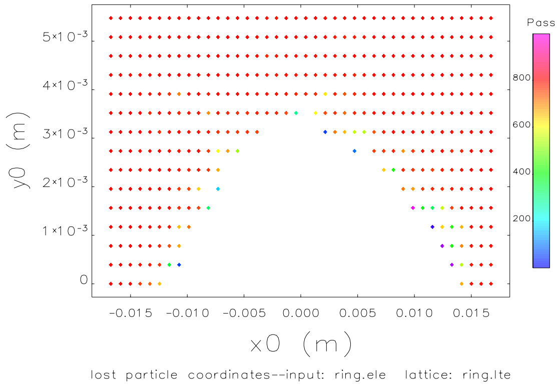

Figure 4. The dynamic aperture at the injection point.

3.2 RF cavity parameters design

We use three RF cavities (one basic and two harmonic cavities) to design long-short bunch operation mode. These RF parameters should meet the requirement of the energy loss supplementation, long bunch for the STCF collision mode and short bunch for the THz mode. The harmonic number of the STCF is an even number, so we can obtain the operating mode with two kinds of bunch lengths, as that reported in BESSY-II [12]. The designed two harmonic cavities are N-th harmonic and $(M + 1/2)$-th harmonic of the basic RF cavity, where M and N are two integers. Under this condition, the sum voltage gradient of the three RF cavities is large at one position (for short bunch) and is small in another position (for long beam). If the harmonic numbers are fixed, only the phase and voltage of the cavities can be varied to obtain the expected bunch lengths when satisfying the synchrotron radiation loss and stable buckets at the two bucket positions. So that the original 958 beam buckets are filled with two kinds of beam bunches, which is the long-short bunch length operation mode.

In this design the constraints are as follows. The energy supplementation at the long and short bunch position should meet the requirement of energy loss per turns. For this facility the energy loss of one particle per turn is 8.2169 keV at 1 GeV energy. At the positions $2K \times 0.5999775$ m, the sum of RF cavity voltage gradient should satisfying the short bunch length requirement. At the positions $(2K + 1) \times 0.5999775$ m, the sum of RF cavity voltage gradient should satisfying the long bunch length requirement. For comparison of the coherent radiation power we designed two versions of short bunches. The first version of the short bunch is 1.5 mm, long bunch is 1.2 cm. The second version of the short bunch length is 2.0 mm, long bunch length is still 1.2 cm. With these constraints we obtain the RF cavity parameters of these two versions, they are listed in table 1 and table 2.

Table 1. RF cavity parameters of 1.5 mm short bunch version.

parameters	Basic cavity	2.5-Harmonic cavity	1.5-Harmonic cavity
Voltage (V)	−735886.16061	−817063.85692	819791.35979
Phase (radian)	−0.01117	−0.01058	−0.01055
Frequency (MHz)	499.672680	1249.182097	749.509258

2022 JINST 17 T01006

Table 2. RF cavity parameters of 2.0 mm short bunch version.

parameters	Basic cavity	2.5-Harmonic cavity	1.5-Harmonic cavity
Voltage (V)	−397132.54367	−26780.50027	273822.26449
Phase (radian)	−0.02069	0.31809	3.111
Frequency (MHz)	499.672680	1249.182097	749.509258

The three cavity voltages and the sum voltage of these two versions are plotted in figure 5. From figure we see that the sum voltage gradient is large at the positions $2K \times 0.5999775$ m, this is corresponding to the short bunch positions. We also see that, the sum voltage has some small slope positions located at the positions $(2K + 1) \times 0.5999775$ m. These are corresponding to the long bunch positions.

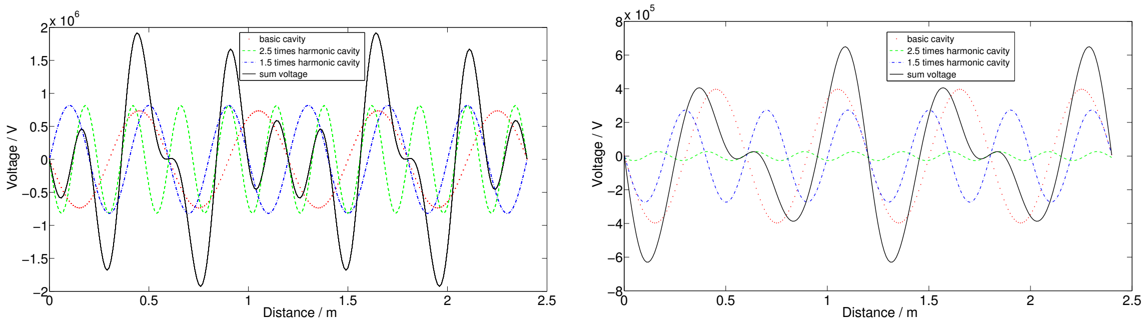

Figure 5. Three RF cavity voltages and the sum voltage of the long-short bunch length operation mode. The left picture corresponding to the short bunch length 1.5 mm mode and the right picture corresponding to the short bunch length 2.0 mm mode.

3.3 Bunch length simulation

In the previous subsection we used the theoretical formula to designed two versions of long-short bunch length operation mode. In this subsection we will install these RF cavities to the above lattice structure and simulate the bunch length evaluation process. The beam size evolution process is simulated by ELEGANT program [13]. Results are shown in figure 6. A Gaussian-distributed beam with 5000 particles per bunch is tracked for 40, 000 turns. Since the longitudinal damping time of this storage ring is 29.12 ms and the circumference of the storage ring is 574.78 m, the tracked turns are equivalent to about 3 times of the damping time. In this simulation only the balance between radiation damping and quantum excitation are considered, while ignoring the interaction force between particles in a bunch. Therefore, in order to save the tracking time 5000 particles are used for simulation but not the real particle numbers per bunch. From figure 6 we see that the simulated bunch length agrees well with the theoretical calculation. One version of the bunch length is stabilized at 1.5 mm and another version is stabilized at 2.0 mm.

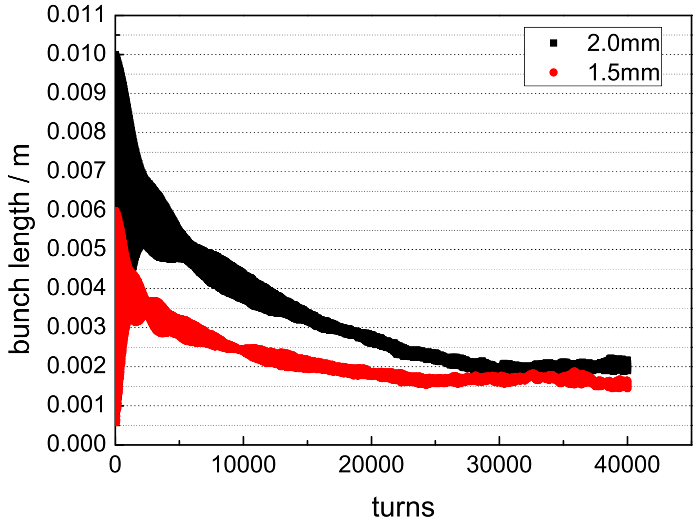

Figure 6. The bunch length damping process for 1.5 mm and 2.0 mm short bunch.

4 Beam properties of the coherent THz radiation mode

4.1 Coherent synchrotron radiation instability

In this sub section we studied the microwave instability driven by the impedance due to the Coherent Synchrotron Radiation (CSR). For electrons, circulating on a circle with radius ρ, the longitudinal wakefield generated by the steady CSR in free space with distance z from the bunch was given by Murphy and so on [14],

$$W_{\mathrm{csr}}(z) = -\frac{4\pi\rho^{1/3}}{(3z)^{4/3}}. \tag{4.1}$$

where z is the longitudinal coordinate relative to the reference particle, and $W(z) = 0$ for $z < 0$. It means that unlike a conventional wake, the CSR force is acting on the electron ahead. Actually the corresponding impedance was already found by Faltens and Laslett in 1973,

$$Z_{\mathrm{csr}}(k) = \left(\frac{2\pi}{c}\right)\frac{\Gamma(2/3)(\sqrt{3}+i)}{3^{1/3}}(\rho k)^{1/3}. \tag{4.2}$$

where k is the wave number of perturbation, Γ is the complete gamma function. Using $\hat{Z}_{\mathrm{csr}}(k) = Z_{\mathrm{csr}}(k)/2\pi\rho$ Stupakov and Heifets analyzed the dispersion relation of the CSR impedance [15]. Results show that for high frequency perturbation $\mathrm{Im}(\omega) < 0$ area ($\omega/c = k$ is the normalized frequency), the beam is naturally stable because the Lamdau damping. Furthermore, the exact impedance for a pipe with aperture b was carried out by Bassi [16]. Cai [17] using the same scaling property to the CSR impedance, and analyzed the stability condition with shielding. As reported in ref. [17] the threshold of instability becomes a function of the shielding parameters $\chi = \sigma_z\rho^{1/2}/b^{3/2}$, and the simplified threshold of the instability has a linear relation to the shielding parameter as follows,

$$\xi^{\mathrm{th}}(\chi) = 0.5 + 0.34\chi. \tag{4.3}$$

It verified that when $\chi > 2$ the coasting beam theory is well fitted for the simulation. Additionally, based on the coasting beam theory the corresponding beam current threshold of CSR instability is

$$I_b > \frac{3\sqrt{2}\alpha\gamma\sigma_\delta^2 I_A \sigma_z}{\pi^{3/2} b}. \tag{4.4}$$

where σ_δ is the RMS energy spread, $I_A = 17.5$ kA is the Alfven beam current, σ_z is the bunch length. This instability result is experimentally confirmed at NSLS VUV ring [8].

For $\chi < 2$ the bunched beam theory works well and the beam becomes unstable when

$$I_b > \frac{8\pi^2 \xi^{\text{th}}(\chi)\sigma_z^{7/3} V_{\text{rf}} \cos\phi_s f_{\text{rf}} f_{\text{rev}}}{c^2 Z_0 \rho^{1/3}}. \tag{4.5}$$

where V_{rf} is the voltage of RF cavity, ϕ_s is the synchrotron phase, f_{rf} is frequency of RF cavity, f_{rev} is revolution frequency. This instability result is measured at different momentum compaction factors with the same RF voltage at ANKA [18].

Using the above formula we calculated the beam CSR instability current threshold for the long and short bunch of this STCF facility. In our calculation $b = 1$ cm, $\rho = 9.55$ m, $\alpha = 0.000898$, $\sigma_\delta = 0.0002659$. Because of the relatively large radius of this storage ring, the shielding parameter χ is larger than 2. So that the formula 4.4 is used to calculate the beam current threshold. Results are given in table 3.

Table 3. Beam current threshold restricted by CSR instablity for different bunch lengthes.

Bunch length σ_z	Shielding parameter χ	Single beam current I_b	Particles per bunch N_b
1.2 cm	61.8	3.23 mA	3.83×10^{10}
1.5 mm	4.6	0.24 mA	2.87×10^{9}
2.0 mm	6.2	0.32 mA	3.83×10^{9}

Since the shielding parameter χ is close to 2 for the 1.5 mm and 2 mm short bunches, we also used the bunched beam theory (formula 4.5) to calculated the current threshold. The result of beam current threshold is very close to the that calculated by the above costing beam theory.

4.2 Touschek lifetime

Touschek lifetime of a synchrotron results from large angle Coulomb scattering can transfer the radial momentum to the longitudinal plane and cause beam loss. The emittance of this lattice is 1nmrad at the energy 1 GeV. In such a small emittance, Touscheck lifetime is the domain lifetime of the storage ring and is a function of energy acceptance. Energy acceptance is dependent on RF cavity and the nonlinear dynamics of the storage ring. The energy acceptance along the half storage ring tracked by ELEGANT program is drawn in figure 7. The Touschek lifetime is calculated using the above energy acceptance data and the particle number given in table 3 which restricted by CSR instability. Result show that the Touschek lifetime is about 176.8 seconds for 1.5mm mode and 138.8 seconds for 2.0mm mode.

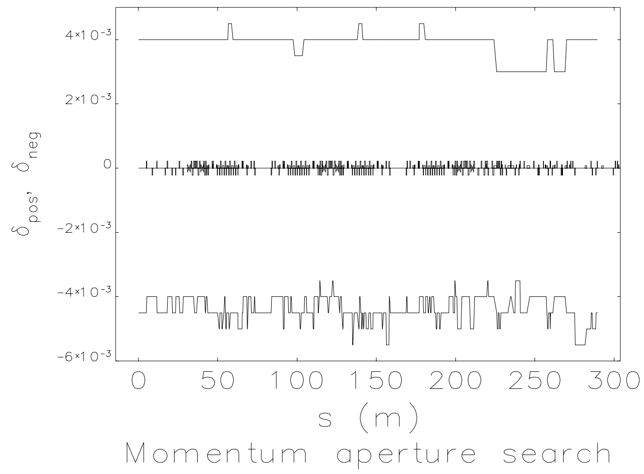

Figure 7. Momentum aperture of the half storage ring.

4.3 Coherent synchrotron radiation power

When the bunch length is shorter than radiation wavelength the synchrotron radiation power is enhanced obviously. The radiation power including coherent and incoherent radiation from bending magnets is expressed by the following formula (4.6) [19, 20].

$$P_{\text{total}} = P_{\omega}\left[N + N\left(N-1\right)g^{2}\left(\lambda,\vec{r}\right)\right]. \tag{4.6}$$

N is the number of particles per bunch, $g\left(\lambda,\vec{r}\right) = |\int e^{ik\vec{r}\cdot\hat{n}}\psi(\vec{r})d\vec{r}|$ is the form factor and $\psi(\vec{r})$ is the three dimension normalized particle distribution. We assume that the beam distribution is Gaussian distribution with RMS bunch length σ_z such that $g\left(\lambda,\sigma_z\right) = \exp(-2\pi^2\sigma_z^2/\lambda^2)$. $P_\omega = \frac{P_\gamma}{\omega_c}S(\frac{\omega}{\omega_c})$ is the power spectrum. P_γ is the single particle radiation power integrated over all of the radiation frequencies. $\omega_c = \frac{3}{2}\frac{c\gamma^3}{\rho}$ is called the critical frequency. The spectral function $S(\frac{\omega}{\omega_c})$ can be expressed by $S(\xi) = \frac{9\sqrt{3}}{8\pi}\xi\int_{\xi}^{\infty}K_{5/3}(\bar{\xi})d\bar{\xi}$, where $K_{5/3}$ is a modified Bessel function. From formula (4.6) we see that the enhancement of the coherent power compared to the incoherent power increases with the electron number N. By using this formula, we calculated the radiation power with different radiation frequency of one short bunch which is plotted in figure 8.

From the result we see that the radiation power can be coherently radiated at THz frequency regions when the bunch length is 1.5 mm or smaller. However, the 2.0 mm bunch length is hard to get a satisfactory coherent THz radiation power in this machine. The radiation power is reduced nearly to the order of incoherent power at THz regions when the bunch length is longer than 2.0 mm. So that, the first version of the long-short bunch length operation RF parameters are preferred.

5 Summary and outlook

In summary, the possibility of coherent THz radiation on a STCF project at the synchrotron radiation mode is discussed. In the synchrotron radiation mode both the long and short bunches are injected simultaneously. The short bunch will radiate coherent THz and the long bunch will increase the beam current. Main performances of the beam including dynamic aperture, momentum aperture,

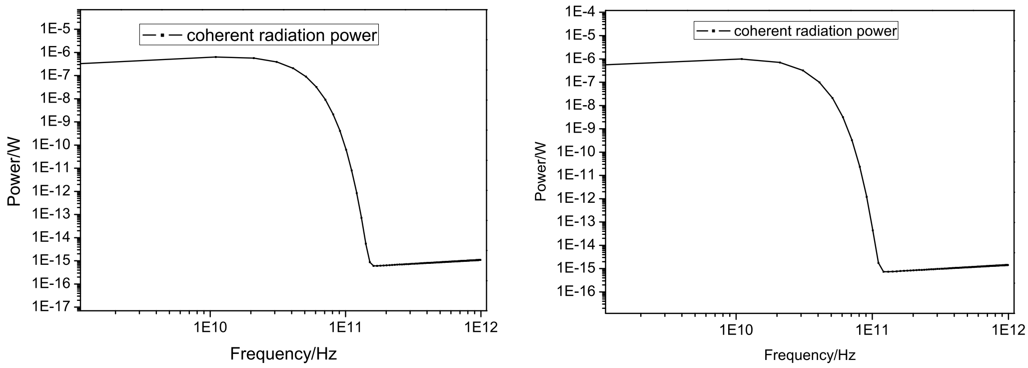

Figure 8. The total radiation power from a short bunch, left plot is the radiation power from 1.5 mm bunch length, right plot is the radiation power from 2.0mm.

Touscheck lifetime, instability and radiation power are simulated. Results show that, in this STCF project it is hard to get a satisfactory radiation power at THz region with 2.0 mm short bunch. To get a satisfactory radiation power the bunch length should be minimized to 1.5 mm or smaller.

There have also some problems to be overcome for achieving THz radiation wave with satisfactory radiation power. The first one is the beam current threshold restricted by CSR impedance for the short bunches. Result show that if the particle numbers per bunch increased to 10^{10}, the coherent radiation power at the THz spectrum can reach to mW. This issue may be solved by the recent proposed scheme low-power feedback loop [21] at SOLEIL storage ring. Another issue is how to inject a large number of particles in a short bunch. To accumulate more particles, we plan to use an off-energy off-axis pulsed multipole injection scheme. The off-energy beam is off-axis injected into the acceptance of the storage ring with one or several pulsed multipole kickers meanwhile the stored beam will be almost unaffected during the injection.

Acknowledgments

This work is supported by the Natural Science Foundation of Fujian Province (grant number 2018J01586 and 2019J01785), Fujian Education Department Funds (grant number JAT200355), National Natural Science Foundation of China (U1832168), the Double First-Class university project foundation of USTC and the research foundation of Fujian University of Technology (grant number GY-Z20163).

References

[1] Y. Yang, Y. Yamagami, X. Yu, P. Pitchappa, J. Webber, B. Zhang et al., *Terahertz topological photonics for on-chip communication*, Nat. Photon. **14** (2020) 446.

[2] Y. Ghasempour, R. Shrestha, A. Charous, E. Knightly and D.M. Mittleman, *Single-shot link discovery for terahertz wireless networks*, Nat. Commun. **11** (2020) .

[3] P. Planken, *A terahertz nanoscope*, Nature **456** (2008) 454.

[4] K.J.P. Jacobs, H. Murakami, F. Murakami, K. Serita, E. Beyne and M. Tonouchi, *Characterization of through-silicon vias using laser terahertz emission microscopy*, Nat. Electron. **4** (2021) 202.

2022 JINST 17 T01006

[5] D. Wang, Y. Zhang, J. Han, X. Li, X. Chen, T. Qiu et al., *Quantification of triglyceride levels in fresh human blood by terahertz time-domain spectroscopy*, *Sci. Rep.* **11** (2021) 13209.

[6] H. Xu, L. Yan, Y. Du, W. Huang, Q. Tian, R. Li et al., *Cascaded high-gradient terahertz-driven acceleration of relativistic electron beams*, *Nat. Photon.* **15** (2021) 426.

[7] G.L. Carr, M.C. Martin, W.R. McKinney, K. Jordan, G.R. Neil and G.P. Williams, *High-power terahertz radiation from relativistic electrons*, *Nature* **420** (2002) 153.

[8] G. Carr, S. Kramer, J. Murphy, R. Lobo and D. Tanner, *Observation of coherent synchrotron radiation from the NSLS VUV ring*, *Nucl. Instrum. Meth. A* **463** (2001) 387.

[9] J.Q. Lan, Q. Luo, C. Zhang, W.W. Gao, Y. Xu and Y. Bai, *Design of beam optics for a Super Tau-Charm Factory*, 2021 *JINST* **16** T07001.

[10] M. Sands, *The Physics of Electron Storage Ring. An Introduction*, Tech. Rep., SLAC-121 (1970).

[11] W. Gao, L. Wang and H. Li, *Multiple-bunch-length operating mode design for a storage ring using hybrid low alpha and harmonic cavity method*, *Nucl. Instrum. Meth. A* **848** (2017) 39.

[12] G. Wüstefeld et al., *Simultaneous long and short electron bunches in the Bessy II storage ring*, in *Proceedings of IPAC*, San Sebastián, Spain, 4–9 September 2011, pp. 2936–2938.

[13] M. Borland, *User's Manual for elegant*, Program version 29.1.0 (2016).

[14] J.B. Murphy, S. Krinsky and R.L. Gluckstern, *Longitudinal wake field for an electron moving on a circular orbit*, *Part. Accel.* **57** (1997) 9.

[15] S. Heifets and G. Stupakov, *Beam instability and microbunching due to coherent synchrotron radiation*, *Conf. Proc. C* **0106181** (2001) 1856

[16] G. Bassi, J.A. Ellison, K. Heinemann and R. Warnock, *Microbunching Instability in a Chicane: Two-Dimensional Mean Field Treatment*, *Phys. Rev. ST Accel. Beams* **12** (2009) 080704.

[17] Y. Cai, *Theory of Microwave Instability and Coherent Synchrotron Radiation in Electron Storage Rings*, Tech. Rep., SLAC-PUB-15243 (2012).

[18] M. Klein et al., *Studies of Bunch Distortion and Bursting Threshold in the Generation of Coherent THz-Radiation at the ANKA Storage Ring*, in *Proceedings of PAC09*, Vancouver, Canada, 4–8 May 2009, pp. 4761–4763.

[19] M. Abo-Bakr, J. Feikes, K. Holldack, G. Wustefeld and H.W. Hubers, *Steady-State Far-Infrared Coherent Synchrotron Radiation detected at BESSY II*, *Phys. Rev. Lett.* **88** (2002) 254801.

[20] A.W: Chao and M. Tigner, *Handbook of Accelerator Physics and Engineerin*, World Scientific (1998).

[21] C. Evain et al., *Coherent Terahertz synchrotron radiation mastered by controlling the irregular dynamics of relativistic electron bunches*, *Nat. Phys.* **15** (2019) 635 [`arXiv:1810.11805`].

2022 JINST 17 T01006